LiSICON – ionic liquid electrolyte for lithium ion battery

Hyea Kim [a], Yi Ding [b], Paul A. Kohl [a,*]

[a] School of Chemical and Biomolecular Engineering, Georgia Institute of Technology, Atlanta, GA 30332-0100, United States
[b] US Army RDECOM-TARDEC, AMSRD-TAR-R, MS 159, 6501 E. 11th Street, Warren, MI 48397-5000, United States

ARTICLE INFO

ABSTRACT

Current lithium-ion batteries (LiB) have limited usefulness in high temperature applications due to the flammability of the organic electrolyte. Alternatively, solid electrolytes can mitigate safety issues and enable high temperature applications. Here, a new solid-state lithium ion battery design is investigated using LiSICON as the electrolyte. To reduce the interfacial resistance between the solid electrolyte and graphite electrode, an ionic liquid was used as the ionic conductor. N-propyl-N-methylpyrrolidinium bis(fluorosulfonyl)imide ($PYR_{13}^+FSI^-$) was used as the ionic liquid due to its high efficiency for lithiation/delithiaion. The cell capacity and efficiency was measured at temperatures from 25 °C to 120 °C. The lithium salt concentration in the ionic liquid was found to change the electrolyte reduction potential. A stable solid electrolyte interface (SEI) was achieved by adjusting the lithium salt concentration in the wetting agent. Impedance spectroscopy was performed to study the cell behavior with different Li salt concentrations at elevated temperature. A carbon anode in a LiSICON cell with 0.75 M $LiTFSI/PYR_{13}^+FSI^-$ had a capacity of 325 mAh g^{-1} and coulombic efficiency of 99.8% during cycling at 80 °C.

© 2011 Elsevier B.V. All rights reserved.

1. Introduction

The state-of-the-art lithium ion batteries (LiB) are used to power portable electronics such as laptops and cell phones. Current LiB research is focused on the development of higher capacity electrode materials including silicon [1–3] to meet the need for higher energy density. Another research goal is to develop safer electrolytes because current LiB uses flammable organic solvents. The limited operation temperature (<50 °C) of the current LiB can be improved by replacing the organic solvent electrolyte.

Solid-state lithium batteries using a solid-state electrolyte are attractive because they can provide safe transport of lithium ions between the anode and cathode by eliminating the organic solvent. Among the various types of solid electrolytes, lithium super ionic conductor (LiSICON) based inorganic lithium-ion conductors have desirable attributes including high lithium ion conductivity (>10^{-3} S cm^{-1} at 25 °C) and wide electrochemical stability windows [4–6]. They can potentially provide high capacity by using a lithium-metal anode, since the solid electrolyte mitigates bridging of dendrites between the anode and cathode. The LiSICON cell can also operate at higher temperature due to its thermal stability and near-zero vapor pressure. In addition, LiSICON is water stable, so a variety of cathodes, even aqueous cathodes can be envisioned [7,8].

Although many studies have shown that ceramic electrolytes are promising for lithium batteries [9,10], only a few studies on solid state lithium-ion batteries at high temperature have been performed. In previous studies, cells were fabricated by pressing the electrolyte and electrodes into a three-layered pellet [11,12]. The full cells consisted of graphite anode and LiCoO$_2$ cathode showed a moderate charge–discharge capacity and high energy density. However, high temperature operation of the solid-state lithium ion batteries has not been investigated.

In this paper, a new cell design incorporating a fully dense ceramic, LiSICON, is investigated as a lithium-ion battery electrolyte operating at high temperature. In order for LiSICON to interface a carbon anode, the interfacial resistance between the LiSICON and electrode needed to be reduced. An ionic liquid was used as the wetting agent to reduce this interfacial resistance between the LiSICON and the carbon anode. The charge–discharge capacity and efficiency of the anode–electrolyte pairs have been investigated at temperature up to 120 °C. Alternating current (AC) impedance was used to understand the cell behavior. Also, the effect of Li salt concentration in the ionic liquid on the anode performance has been studied.

2. Experimental

The LiSICONs were obtained from Ceramatec (Salt Lake City, Utah). The circular thin-film LiSICON slices had a radius of 2.6 cm and were 500 μm thick. The ionic liquid, N-propyl-N-methylpyrrolidinium bis(fluorosulfonyl)imide ($PYR_{13}^+FSI^-$, 99.9%,

* Corresponding author. Tel.: +1 404 894 2893; fax: +1 404 894 2866.
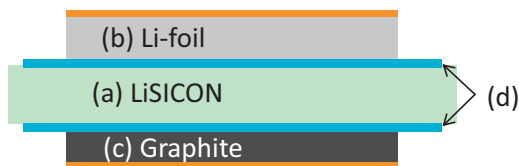 E-mail addresses: kohl@gatech.edu, Paul.Kohl@chbe.gatech.edu (P.A. Kohl).

Fig. 1. A schematic of a half-cell with (a) LiSICON electrolyte using (d) wetting agent for both (b) lithium counter and (c) graphite working electrode.

Solvionic), and lithium bis(triflouromethanesulfonyl)imide (LiTFSI, 99%, Acros) were used inside an inert atmosphere glovebox. LiTFSI was dissolved in the $PYR_{13}^{+}FSI^{-}$ and used as a wetting agent (LiTFSI/$PYR_{13}^{+}FSI^{-}$). Commercial graphite electrodes were purchased from MTI Corp. The electrode sheet is based on 9 μm thick copper sheet coated with carbonaceous mesophase spherules (CMS) graphite with a density of 120 g m^{-2}. The binder was styrene butadiene rubber (SBR) and carboxymethyl cellulose (CMC). The reversible capacity of the electrode is 330 mAh g^{-1}.

Half-cells were constructed to be used in charge–discharge cycling experiments with Li foil as a counter/reference electrode. The electrode sheet was cut into squares, 0.81 cm^2 in area, for use as the working electrode. On each side of the LiSICON, was placed a piece of fiber glass (Whatman, GF/D) soaked with 250 μL of wetting agent, LiTFSI/$PYR_{13}^{+}FSI^{-}$. The electrodes were placed on top of the fiber glass and allowed to equilibrate for at least 4 h to ensure the graphite particles were soaked with the wetting agent. Equilibrium was confirmed by AC impedance. The cross section of the cell is shown in Fig. 1.

All work was performed in an argon filled Vacuum Atmospheres glovebox. Electrochemical experiments were carried out with an Arbin battery test system. Cycling tests were performed between 2.5 and 0.001 V vs Li/Li$^+$ (V) in galvanostatic mode with charge and discharge currents at C/20. The coulombic reversibility of the cells was tested by cyclic voltammetry (CV) measurements between 2.5 and 0.001 V vs lithium metal reference electrode at a scan rate of 1 mV s^{-1}. The cells were evaluated with the C-rate test by varying only the discharge current from C/20 to 1 C. AC impedance was performed with a Perkin Elmer Parstat Model 2263. The frequency of the impedance measurements ranged from 10 Hz to 500 kHz with an AC signal amplitude of 10 mV.

3. Results and discussion

The goal of this work was to investigate a solid-state electrolyte lithium-ion anode capable cycling at elevated temperature. In previous studies, electrodes for solid-state lithium ion batteries were pressed into pellets [11,12]. To maximize the electrode utilization, about 50% of the solid electrolyte material was incorporated into the active material (graphite). This resulted in incomplete utilization of the active material, thus lowering the energy density. Also, there is a possible mismatch in the coefficient of thermal expansion between the active material and solid electrolyte, raising questions about the long-term stability of these materials. In the design investigated here, prepared graphite anodes were used.

The first step was to measure the capacity of the graphite electrodes (MTI Corp.) with a conventional organic solvent electrolyte (1.0 M LiPF$_6$/EC-DMC (1:1 vol%)). Fig. 2 shows three charge–discharge cycles for the graphite electrodes with an organic solvent electrolyte. The first charge capacity was 371 mAh g^{-1}, which is very close to the theoretical capacity of graphite (375 mAh g^{-1}). The first discharge capacity was 325 mAh g^{-1}, indicating 46 mAh g^{-1} of capacity was irreversible and could have contributed to the formation of a solid electrolyte interface (SEI) layer [13,14]. The charge–discharge efficiency in the second cycle was 97%.
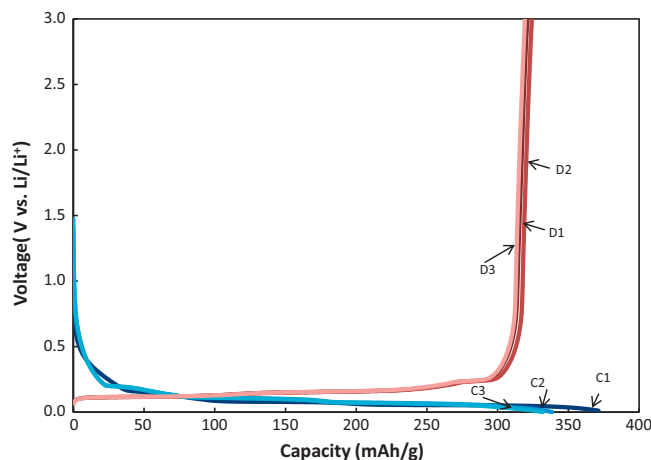

Fig. 2. First three charge–discharge curves for the half-cell using organic solvent electrolyte (1.0 M LiPF$_6$/EC-DMC (1:1)) with a commercial graphite electrode (Cx: xth charge curve, Dx: xth discharge curve).

When the organic solvent was replaced with LiSICON and the graphite was pressed against the LiSICON, it was not possible to lithiate/delithiate the electrode. The low current density with a LiSICON/graphite electrode was reflected in the CV. The current was much lower than the current density observed with a liquid electrolyte and no lithiation/delithiaion peaks were observed. The cause of the poor performance is the lack of ionic conductivity between the graphite electrode and the LiSICON. A large series resistance value of ca. 10^4 Ω was observed in the AC impedance study.

An ionic wetting agent was used to reduce the interfacial resistance between the solid electrodes and solid LiSICON. A conventional organic solvent can be used as the wetting agent, however, that would reintroduce flammability and temperature constraints. Ionic liquids have been studied as an alternative electrolyte for LiB [15–20]. Li salts, such as LiPF$_6$ or LiTFSI, can be dissolved in an ionic liquid to serve to complete the lithium ion pathway between the LiSICON and graphite. In addition, the ionic liquid can be selected so as to have a very wide operating temperature range, wide electrochemical window and near-zero vapor pressure. Ishikawa et al. [21,22] reported that FSI$^-$ based ionic liquids showed reversible lithiation without using an SEI forming agent. $PYR_{13}^{+}FSI^{-}$ was chosen here as the wetting agent, and LiTFSI was used as the lithium salt in the ionic liquid due to the anion similarity.
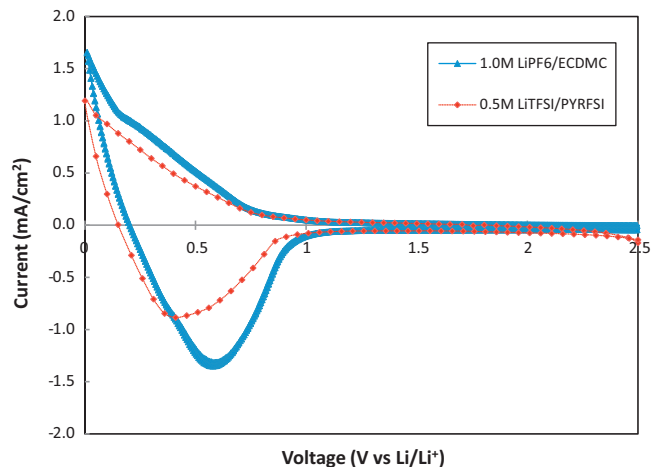

Fig. 3. Cyclic voltammetry of the cell with 0.5 M LiTFSI/$PYR_{13}^{+}FSI^{-}$, comparing to the cell with 1.0 M LiPF$_6$/EC-DMC as an electrolyte, at 25 °C, 1 mV s^{-1}.

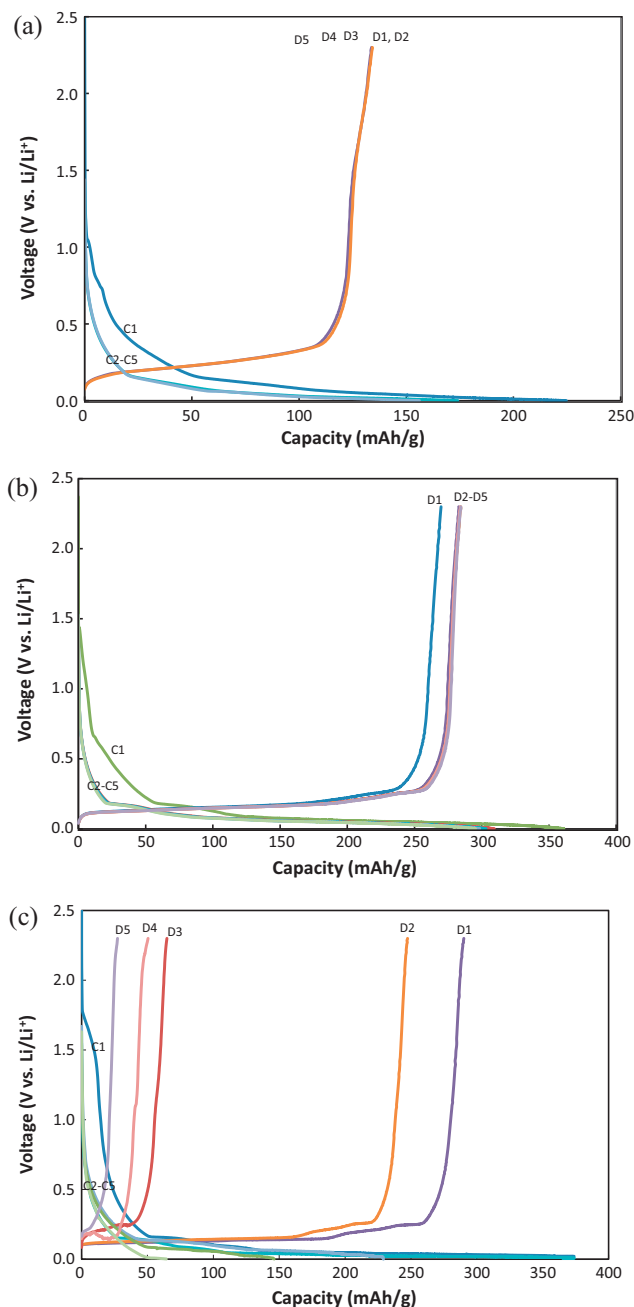**Fig. 4.** First five charge–discharge curves of the cells at (a) 50 °C, (b) 80 °C, and (c) 120 °C, with LiSICON using 1.0 M LiTFSI/PYR$_{13}^+$FSI$^-$ as a wetting agent.
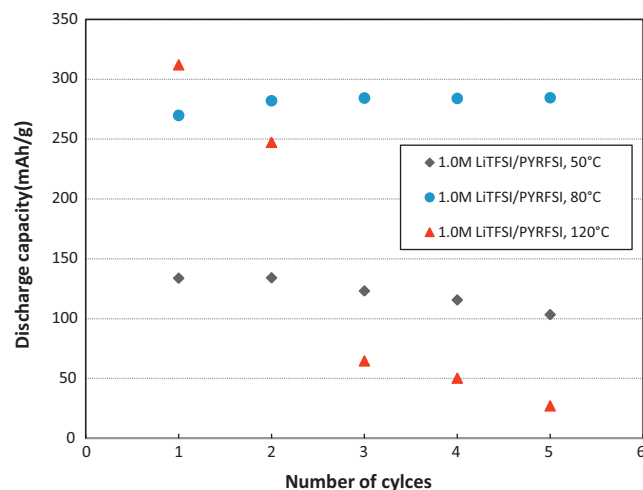

Fig. 5. Comparison of the discharge capacity for the five charge–discharge cycles at different temperatures in Fig. 4, at C/20.

the lower viscosity and higher conductivity of the ionic liquid at the higher temperature. The ionic liquid was better able to wet the LiSICON and graphite surfaces leading to an apparent increase in capacity. Capacity fade was observed at 50 °C while at 80 °C the capacity was stable. At 120 °C, the anode showed the highest first-cycle capacity, 312 mAh g^{-1}, however, the performance degraded with cycling. This could be due to the instability of the SEI at temperatures above 100 °C [23].

The first-cycle charging curves for the anodes were compared to each other in Fig. 6 to better evaluate the cell behavior at elevated temperatures. Two significant differences occurred at high temperature. First, the electrolyte reduction potential shifted slightly toward positive potentials with temperature, with respect to the lithium reference electrode. This is probably due to the accelerated SEI formation due to electrolyte reduction at more positive potentials at higher temperature [24]. Second, the lithiation process was more facile at higher temperature resulting in a higher first-cycle capacity. The first-cycle charge capacities were 57, 218, and 359 mAh g^{-1} at 25 °C, 50 °C, and 80 °C, respectively. This increase is a reflection of the cut off potential limit for the cycling (0 V vs Li/Li$^+$) where poor electrode or LiSICON wetting, or lower conductivity would lead to a higher iR drop in the electrolyte at low temperature resulting in an apparent reduction in capacity.
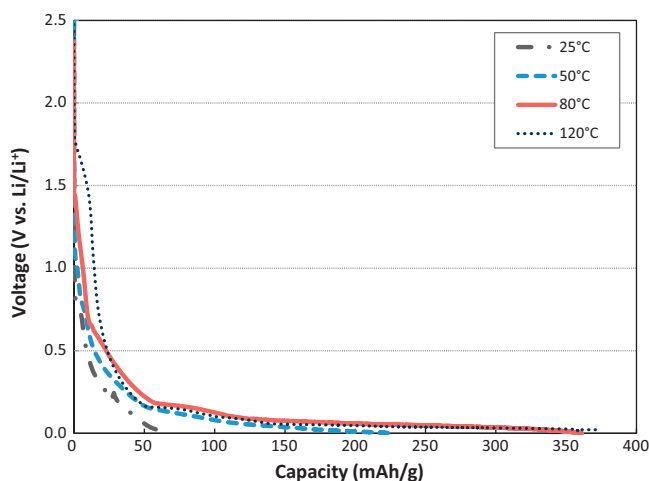
Fig. 3 shows the CV for 0.5 M LiTFSI/PYR$_{13}^+$FSI$^-$ and 1.0 M LiPF$_6$/EC-DMC as the electrolyte (without LiSICON) for a graphite electrode at room temperature. A clear lithiation reduction current and delithiation oxidation peak was observed. The coulombic efficiency for delithiation/lithiation was 84% compared to 97% with the organic solvent.

The 1.0 M LiTFSI/PYR$_{13}^+$FSI$^-$ ionic liquid was used as a wetting agent between LiSICON and graphite. The charge–discharge behavior for repetitive cycling (five cycles) at C/20 rate was performed at 50 °C, 80 °C and 120 °C, Fig. 4(a–c). A summary of the discharge capacity is shown in Fig. 5. At 50 °C, Fig. 4a, the capacity of the first and second discharge was 134 mAh g^{-1}, and the capacity decreased gradually with increasing cycling. At 80 °C, the discharge capacity for the first cycle was double that of the 50 °C experiment, and increased to 285 mAh g^{-1} by the third cycle. This is likely due to

Fig. 6. Comparison of the first charge curves at different temperatures in Fig. 4.
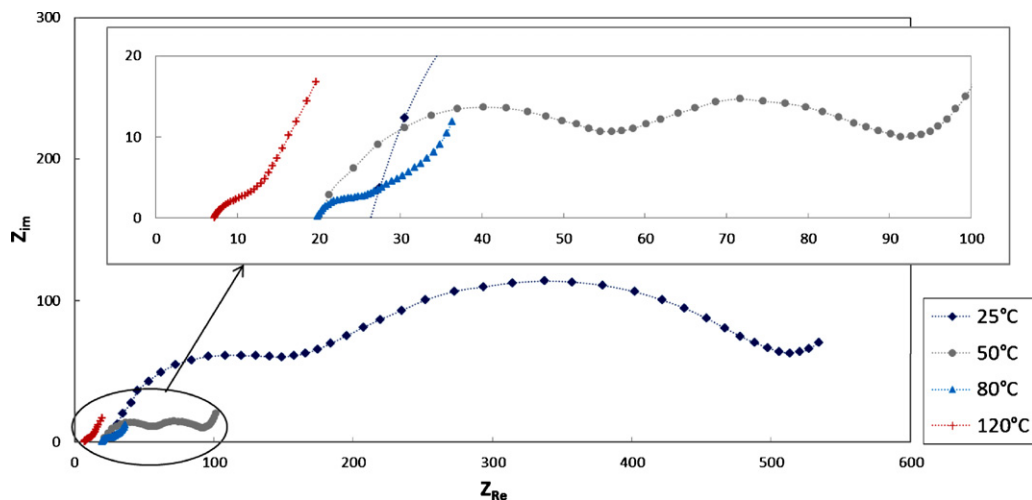
Fig. 7. Naquist plot at elevated temperatures of the cell with LiSICON using 1.0 M LiTFSI/PYR$_{13}$$^+FSI^-$ as a wetting agent.

Impedance analysis was carried out to study changes in resistance of the cells with temperature. The Nyquist plot for the cells at 25 °C, 50 °C, 80 °C, and 120 °C are shown in Fig. 7. Two arcs appeared at 25 °C with a high resistance over 500 Ω. The capacitance of the two arcs was calculated assuming a parallel resistance (R_{ct}) capacitance (C) model, Eq. (1) where ω is the frequency.

$$C[F] = \frac{1}{\omega R_{ct}} \qquad (1)$$

At high frequency, the first arc has a capacitance value of ca. 10^{-8} F and is most likely due to the RC circuit for LiSICON grain boundaries [25]. The second arc at low frequency had a capacitance value of ca. 10^{-6} F. It corresponds to typical double layer capacitance values and should be the sum of the two electrodes, lithium counter and graphite electrode.

As the temperature increased from 25 °C to 120 °C, the high frequency x-axis intercept decreased from 27.5 to 7.2 Ω. This value corresponds to the bulk electrolyte resistance (R_b), indicating that the resistance of the LiSICON and the wetting agent, 1.0 M LiTFSI/PYR$_{13}$$^+FSI^-$, became smaller with temperature. Moreover, the charge-transfer resistance (R_{ct}), difference between the x-axis intercept for the low frequency arc, decreased significantly from 434.6 Ω at 25 °C to 5.8 Ω at 120 °C, indicating better wetting of the surfaces at higher temperature. Also, the grain boundary arc disappeared temperatures above 80 °C, indicating the grain boundary resistance is negligible. The impedance results support the results shown in Figs. 5 and 6.

The effect of the lithium salt concentration on the performance of the ionic liquid was also of interest. It is known that the viscosity of ionic liquid electrolyte increases as the dissolved lithium salt concentration increases [16,17]. Charge–discharge cycling was performed at C/20 with lower LiTFSI concentration in PYR$_{13}$$^+FSI^-$. Fig. 8(a) compares the capacity of the first five discharge cycles for three cells with different LiTFSI concentrations of 0.50 M, 0.75 M,
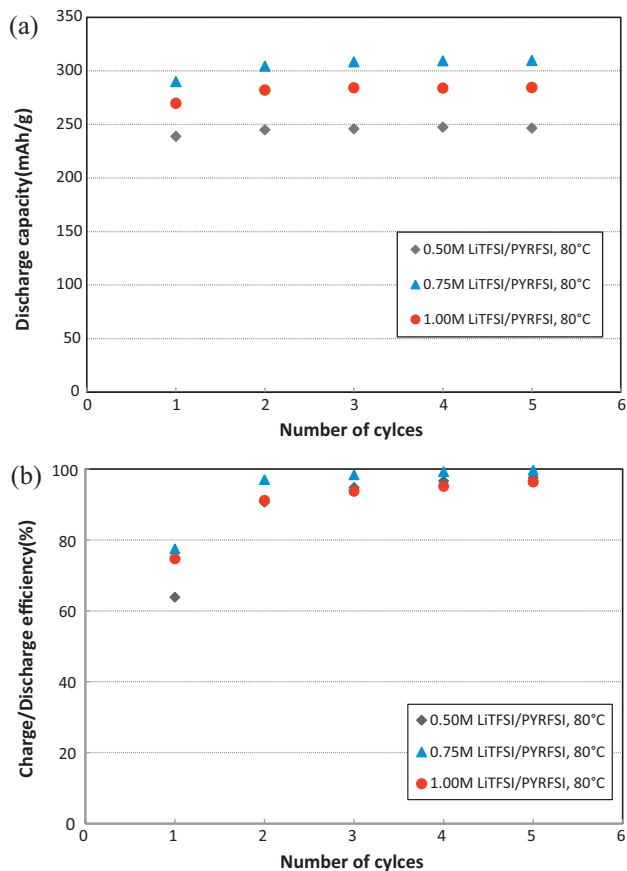

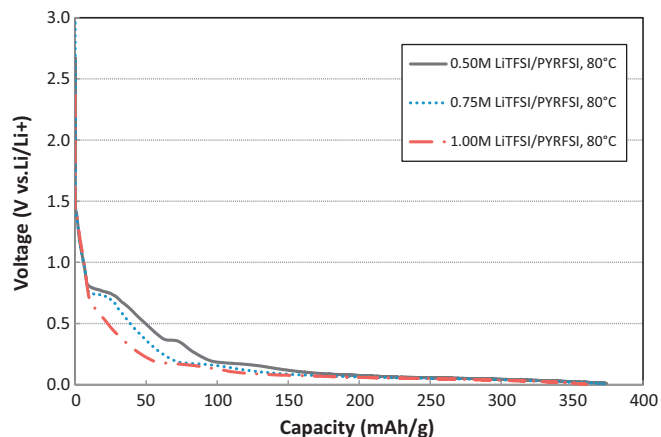**Fig. 8.** The effect of the Li salt concentration in wetting agent on (a) discharge capacity and (b) charge–discharge efficiency for five cycling tests at C/20.

Fig. 9. The effect of the Li salt concentration on the first charge curve (electrolyte reduction potential) at C/20.
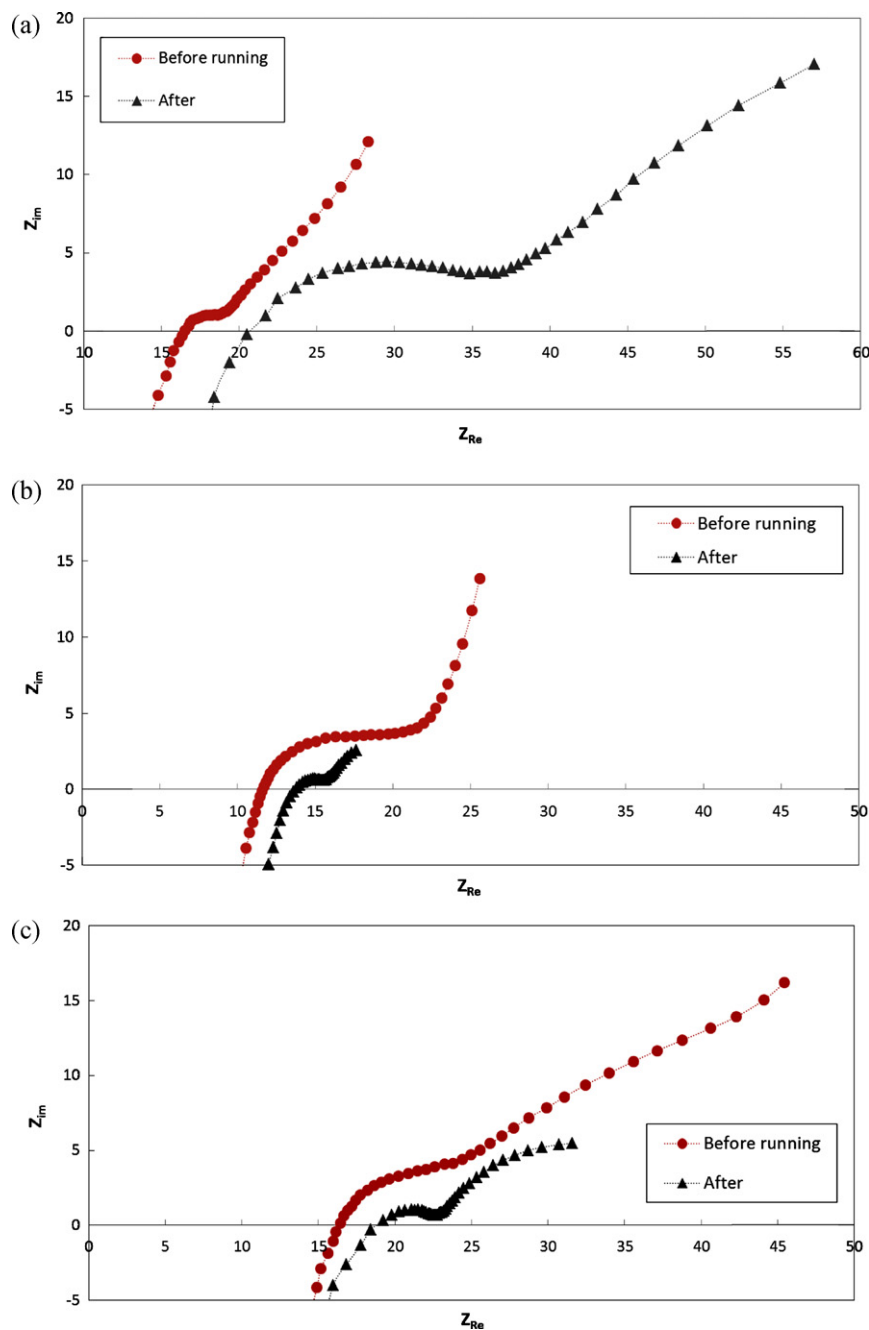
Fig. 10. Naquist plot comparing before and after operating the cells using (a) 0.50 M, (b) 0.75 M and (c) 1.00 M LiTFSI/PYR$_{13}^+$FSI$^-$ as a wetting agent, incorporating LiSICON at 80 °C.

and 1.00 M. The 0.75 M LiTFSI/PYR$_{13}^+$FSI$^-$ ionic liquid provided better performance than the 1.00 M liquid, probably due to the lower viscosity providing better wetting. The first capacity was 290 mAh g^{-1} and increased to 310 mAh g^{-1} by the third cycle. The efficiency of 0.75 M LiTFSI/PYR$_{13}^+$FSI in Fig. 8(b) reached to 99.7% by the fourth cycle, which is higher than the efficiency with organic solvent electrolyte in Fig. 2.

The capacity of the 0.50 M LiTFSI/PYR$_{13}^+$FSI$^-$ ionic liquid was lower by 60 mAh g^{-1} compared to the 0.75 M ionic liquid. Although the 0.50 M LiTFSI/PYR$_{13}^+$FSI$^-$ has lower viscosity and higher conductivity, the first charge/discharge efficiency for 0.5 M in Fig. 8(b) was only 64%, compared to 74% and 77% for 1.00 M and 0.75 M, respectively. This may be due to the efficiency for formation of the SEI, which occurs on the first-cycle. The first-cycle charge curves

were compared to help understand the reason for this lower performance for the 0.50 M ionic liquid.

Fig. 9 compares the first-cycle charging curves as a function of the lithium ion concentration in the ionic liquid. As the lithium concentration was increased from 0.50 M to 1.00 M, the onset potential for reduction shifted from 0.86 V to 0.72 V vs Li/Li$^+$. The more positive reduction potential led to greater electrolyte reduction. The irreversible lithium capacity in 0.5 M during the first-cycle charge–discharge was 135 mAh g^{-1}, which is higher than for 0.75 M (84 mAh g^{-1}) and 1.00 M (91 mAh g^{-1}). A greater quantity of electrolyte reduced on the graphite electrode could form thicker SEI resulting in higher irreversible capacity. In the case of 1.00 M lithium concentration, the first discharge capacity was lower by 15 mAh g^{-1} compared to 0.75 M, probably caused by higher
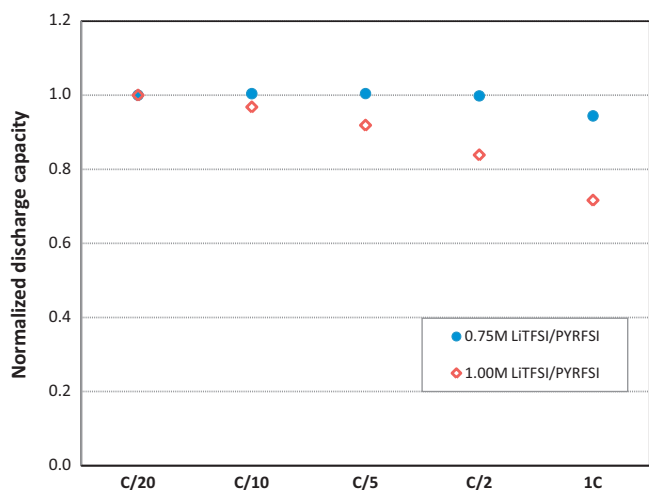
Fig. 11. Rate capability tests for the cells with 0.75 M and 1.00 M LiTFSI/PYR$_{13}^+$FSI$^-$ as a wetting agent, incorporating LiSICON at 80 °C.

viscosity and poorer surface wetting. The capacity of 1.00 M in Fig. 8 was lowered by 25 mAh g^{-1} than 0.75 M for all cycles.

As the electrolyte reduction potential shifted with concentration, SEI formation could affect the cell resistance. The series cell resistance could increase with formation of the SEI layer. Impedance spectroscopy was used to monitor the cell resistance with concentration. Fig. 10 compares the impedance of the electrodes with 0.50 M, 0.75 M and 1.00 M lithium concentration before and after the cycling. In all cases, the bulk resistance increased after cycling the cells. This was possibly due to SEI formation. However, the increase in bulk resistance (4.0 Ω) for 0.5 M lithium concentration was twice to that of the 0.75 M electrolyte (2.2 Ω) and 1.00 M electrolyte (2.0 Ω). This is consistent with a thicker SEI having been formed as a result of the positive shift in electrolyte reduction potential at the lower lithium salt concentration. In addition, the R_{ct} of 0.5 M cell tripled after cycling due to the formation of a thick SEI film. However, the R_{ct} of the 0.75 M and 1.00 M cells decreased.

A higher conductivity and lower viscosity electrolyte is desired as an interface between the LiSICON and graphite electrode. This would likely lead to a higher rate-capability due to more efficient transport of lithium through the electrolyte material [26]. The cells with 0.75 M and 1.00 M lithium ion concentration were evaluated at different C-rates by varying the discharge current from C/20 to 1 C. Fig. 11 shows the capacity as a function of C-rate. The discharge capacity at various C-rates was normalized to the value for C/20 for comparison purposes. The capacity of the 1.00 M cell steadily decreased with C-rate and the capacity at 1 C was only 70% of that at C/20. However, the cell with 0.75 M lithium ionic liquid provided essentially the same capacity up to C/2.

4. Conclusion

A lithium ion anode battery design incorporating a ceramic membrane was investigated. In order for the graphite electrode to undergo lithiation/delithiation, an ionic liquid electrolyte was used between the LiSICON and graphite electrode. PYR$_{13}^+$FSI$^-$ ionic liquid was studied as a lithium ion conducting medium which allowed operation at higher temperatures. At 80 °C, the cell showed a stable discharge capacity, while the cell performance above 100 °C decreased due to the possible decomposition of SEI. Also, it was found that the SEI formation on the graphite electrode was affected by the lithium salt concentration in the ionic liquid. The salt concentration affects the viscosity and conductivity as well as the electrochemical stability window. Finally, the cell with LiSICON electrolyte using 0.75 M LiTFSI/PYR$_{13}^+$FSI$^-$ as the wetting agent showed comparable capacity (310 mAh g^{-1}) to an organic electrolyte. The capacity was stable with cycling and the efficiency was 99.7%.

References

[1] C.K. Chan, H. Peng, G. Liu, K. McIlwrath, X.F. Zhang, R.A. Huggins, Y. Cui, Nat. Nanotechnol. 3 (2008) 31–35.
[2] A. Magasinski, P. Dixon, B. Hertzberg, A. Kvit, J. Ayala, G. Yushin, Nat. Mater. 9 (2010) 353–358.
[3] B. Scrosati, J. Garche, J. Power Sources 195 (2010) 2419–2430.
[4] F. Mizuno, A. Hayashi, K. Tadanaga, M. Tatsumisago, Adv. Mater. 17 (2005) 918–921.
[5] R. Kanno, M. Murayama, J. Electrochem. Soc. 148 (2001) A742–A746.
[6] K. Minami, A. Hayashi, M. Tatsumisago, Solid State Ionics 179 (2008) 1282–1285.
[7] G. Girishkumar, B. McCloskey, A.C. Luntz, S. Swanson, W. Wilcke, J. Phys. Chem. Lett. 1 (2010) 2193–2203.
[8] H. Li, Y. Wang, H. Na, H. Liu, H. Zhou, J. Am. Chem. Soc. 131 (2009) 15098–15099.
[9] R. Kanno, M. Murayama, T. Inada, T. Kobayashi, K. Sakamoto, N. Sonoyama, A. Yamada, S. Kondo, Electrochem, Solid State Lett. 7 (2004) A455–A458.
[10] H. Takahara, M. Tabuchi, T. Takeuchi, H. Kageyama, J. Ide, K. Handa, Y. Kobayashi, Y. Kurisu, S. Kondo, R. Kanno, J. Electrochem. Soc. 151 (2004) A1309–A1313.
[11] Y. Seino, K. Takada, B.C. Kim, L.Q. Zhang, N. Ohta, H. Wada, M. Osada, T. Sasaki, Solid State Ionics 176 (2005) 2389–2393.
[12] K. Takada, T. Inada, A. Kajiyama, H. Sasaki, S. Kondo, M. Watanabe, M. Murayama, R. Kanno, Solid State Ionics 158 (2003) 269–274.
[13] S.S. Zhang, M.S. Ding, K. Xu, J. Allen, T.R. Jow, Electrochem. Solid State Lett. 4 (2001) A206–A208.
[14] F. Kong, R. Kostecki, G. Nadeau, X. Song, K. Zaghib, K. Kinoshita, F. McLarnon, J. Power Sources 97–98 (2001) 58–66.
[15] S. Seki, Y. Kobayashi, H. Miyashiro, Y. Ohno, Y. Mita, N. Terada, P. Charest, A. Guerfi, K. Zaghib, J. Phys. Chem. C 112 (2008) 16708–16713.
[16] A. Guerfi, M. Dontigny, Y. Kobayashi, A. Vijh, K. Zaghib, J. Solid State Electrochem. 13 (2009) 1003–1014.
[17] A. Guerfi, M. Dontigny, P. Charest, M. Petitclerc, M. Lagace, A. Vijh, K. Zaghib, J. Power Sources 195 (2010) 845–852.
[18] V. Baranchugov, E. Markevich, G. Salitra, D. Aurbach, G. Semrau, M.A. Schmidt, J. Electrochem. Soc. 155 (2008) A217–A227.
[19] G.B. Appetecchi, M. Montanino, A. Balducci, S.F. Lux, M. Winterb, S. Passerini, J. Power Sources 192 (2009) 599–605.
[20] S.F. Lux, M. Schmuck, S. Jeong, S. Passerini, M. Winter, A. Balducci, Int. J. Energy Res. 34 (2010) 97–106.
[21] M. Ishikawa, T. Sugimoto, M. Kikuta, E. Ishiko, M. Kono, J. Power Sources 162 (2006) 658–662.
[22] T. Sugimoto, M. Kikuta, E. Ishiko, M. Kono, M. Ishikawa, J. Power Sources 183 (2008) 436–440.
[23] Q.C. Hu, S. Osswald, R. Daniel, Y. Zhu, S. Wesel, L. Ortiz, D.R. Sadoway, J. Power Sources 196 (2011) 5604–5610.
[24] J. Mun, Y.S. Jung, T. Yim, H.Y. Lee, H.J. Kim, Y.G. Kim, S.M. Oh, J. Power Sources 194 (2009) 1068–1074.
[25] J.T.S. Irvine, D.C. Sinclair, A.R. West, Adv. Mater. 2 (1990) 132–138.
[26] K. Zaghib, J. Shim, A. Guerfi, P. Charest, K.A. Striebel, Electrochem. Solid State Lett. 8 (2005) A207–A210.